JOURNAL OF VIROLOGY, Nov. 1998, p. 8586–8596 Vol. 72, No. 11
0022-538X/98/$04.00+0

Protection against Fatal Sindbis Virus Encephalitis by Beclin, a Novel Bcl-2-Interacting Protein

XIAO HUAN LIANG,[1] LINDA K. KLEEMAN,[1] HUI HUI JIANG, GERALD GORDON,[2] JAMES E. GOLDMAN,[3] GAIL BERRY,[2] BRIAN HERMAN,[2]† AND BETH LEVINE[1]*

Departments of Medicine[1] and Pathology,[3] Columbia University College of Physicians and Surgeons, New York, New York 10032, and Department of Cell Biology and Anatomy, University of North Carolina at Chapel Hill, Chapel Hill, North Carolina 27599[2]

Received 5 May 1998/Accepted 6 July 1998

***bcl-2*, the prototypic cellular antiapoptotic gene, decreases Sindbis virus replication and Sindbis virus-induced apoptosis in mouse brains, resulting in protection against lethal encephalitis. To investigate potential mechanisms by which Bcl-2 protects against central nervous system Sindbis virus infection, we performed a yeast two-hybrid screen to identify Bcl-2-interacting gene products in an adult mouse brain library. We identified a novel 60-kDa coiled-coil protein, Beclin, which we confirmed interacts with Bcl-2 in mammalian cells, using fluorescence resonance energy transfer microscopy. To examine the role of Beclin in Sindbis virus pathogenesis, we constructed recombinant Sindbis virus chimeras that express full-length human Beclin (SIN/*beclin*), Beclin lacking the putative Bcl-2-binding domain (SIN/*beclin*ΔBcl-2BD), or Beclin containing a premature stop codon near the 5′ terminus (SIN/*beclin*stop). The survival of mice infected with SIN/*beclin* was significantly higher (71%) than the survival of mice infected with SIN/*beclin*ΔBcl-2BD (9%) or SIN/*beclin*stop (7%) ($P < 0.001$). The brains of mice infected with SIN/*beclin* had fewer Sindbis virus RNA-positive cells, fewer apoptotic cells, and lower viral titers than the brains of mice infected with SIN/*beclin*ΔBcl-2BD or SIN/*beclin*stop. These findings demonstrate that Beclin is a novel Bcl-2-interacting cellular protein that may play a role in antiviral host defense.**

The cellular antiapoptotic gene *bcl-2* represents a novel class of antiviral host defense molecules which function both by restricting viral replication and by preventing virus-induced cell death. Bcl-2 blocks apoptosis in vitro induced by several different RNA viruses, including Sindbis virus (18, 41), influenza virus (13, 26), reovirus (31), Semliki Forest virus (34), LaCrosse virus (29), and Japanese B encephalitis virus (21). Previously, we have shown that Bcl-2 overexpression in virally infected neurons in vivo also protects mice against fatal encephalitis caused by the prototypic alphavirus, Sindbis virus (17). The protective effects of Bcl-2 against fatal Sindbis virus encephalitis were associated with a reduction both in neuronal apoptotic death and in central nervous system (CNS) viral replication. A similar antiviral effect of Bcl-2 overexpression has been observed during Sindbis virus infection in cultured AT3 cells (41) as well as during influenza virus infection of MDCK cells (26), Japanese B encephalitis virus infection of N18 cells (21), and Semliki Forest virus infection of AT3 cells (34). Although the role of endogenous Bcl-2 in antiviral defense has yet to be evaluated, these studies support the hypothesis that Bcl-2 may be important in protecting cells against viral infections.

Most previous studies examining the effects of Bcl-2 on viral infections have been with neurotropic RNA viruses (e.g., Sindbis virus, reovirus, Semliki Forest virus, LaCrosse virus, and Japanese B virus) (18, 21, 29, 31, 34, 41). Although Bcl-2 may affect viral replication and virus-induced apoptosis with non-neurotropic viruses (e.g., influenza virus) (13, 26), host mechanisms to inhibit apoptosis may be of particular importance during viral infections of vital, nonrenewable cell populations such as neurons. In such instances, virus-induced apoptotic death of neurons may result in irreversible CNS pathology and death of the host organism (1, 17, 19, 25). Therefore, while apoptosis in other cell types may be an adaptive host defense strategy that reduces total viral burden for the organism (reviewed in references 11, 16, 36, and 39), unique strategies may have evolved to permit control of CNS viral replication without inducing apoptotic death of infected neurons. It is thus possible that cellular genes that play a role in preventing apoptosis during normal neuronal development (e.g., *bcl-2* and *bcl-x*$_L$) (reviewed in reference 23) may also be important in regulating CNS viral replication and in defending against apoptosis induced by neurotropic viruses.

To further understand how the cellular gene *bcl-2* exerts antiapoptotic and antiviral effects during CNS viral infection, we performed a yeast two-hybrid screen to identify Bcl-2-interacting gene products in adult mouse brain. In this study, we describe the identification of a novel Bcl-2-interacting gene product, which we named Beclin because of its predicted coiled-coil structure (hence, the "-in" suffix) and its interaction with Bcl-2 (Becl). Like Bcl-2 overexpression, Beclin overexpression in neurons in vivo can inhibit Sindbis virus replication, reduce CNS apoptosis, and provide protection against fatal Sindbis virus infection. A Beclin construct lacking the putative Bcl-2-binding domain provides no protection and has no antiviral activity. Thus, our findings identify a novel protein, Beclin, which may play a role in host defense against Sindbis virus infection. In addition, they suggest that interactions with Bcl-

* Corresponding author. Mailing address: Department of Medicine, Columbia University College of Physicians and Surgeons, 630 W. 168th St. P & S 8-444, New York, NY 10032. Phone: (212) 305-7312. Fax: (212) 305-7290. E-mail: Levine@cuccfa.ccc.columbia.edu.

† Present address: Department of Cellular and Structural Biology, University of Texas Health Science Center at San Antonio, San Antonio, TX 78284.

2-like proteins may be important for the protective activity of Beclin.

MATERIALS AND METHODS

Plasmids. To construct vectors for transient expression in mammalian cells, the open reading frame of human *bcl-2*, flag epitope-tagged human *beclin*, and flag epitope-tagged *beclin* deleted of nucleotides 238 to 453 were cloned into pSG5 (Stratagene). To construct viral cDNA clones, the previously described neurovirulent double subgenomic Sindbis virus vector dsTE12 was used (17). Full-length flag epitope-tagged human *beclin*, human *beclin* containing a stop codon inserted at nucleotide position 270, human *beclin* containing an in-frame deletion of nucleotides 238 to 453, human *bcl-2*, and human *bcl-2* containing a stop codon at nucleotide position 118 were cloned into the *Bst*EII site of dsTE12 to generate plasmids SIN/*beclin*, SIN/*beclin*stop, SIN/*beclin*Δbcl-2BD, SIN/*bcl-2*, and SIN/*bcl-2*stop, respectively. To construct vectors for yeast two-hybrid studies, the sequences encoding amino acids (aa) 1 to 218 of human *bcl-2*, 1 to 212 of *bcl-x*$_L$, 1 to 149 of *bcl-x*$_S$, and 1 to 171 of *bax* were cloned into pGBT9 in frame with the GAL4 DNA-binding domain. To avoid difficulties with targeting of proteins to the nucleus, the sequences encoding C-terminal transmembrane domains of *bcl-2* family members were omitted. Control pGBT9 plasmids containing lamin (pLAM5′) and p53 (pVA3) inserts were obtained from Clontech.

Yeast two-hybrid screen. *Saccharomyces cerevisiae* SFY526 cells were cotransformed with pGBT9/*bcl-2* and 10^6 cDNA molecules from an adult mouse brain library fused to a GAL4 activation domain vector (pGAD10; Clontech), plated onto SD medium lacking tryptophan and leucine, incubated at 30°C for 4 days, and then screened for LacZ activity by a colony lift filter assay. Putative interacting clones were isolated by manipulation in *leuB Escherichia coli*, and further tested against pGBT9 and control plasmids. A positive β-galactosidase reaction between pGBT9/*bcl-2* and clone F1 was obtained within 10 to 15 min. For analysis of interactions between Beclin and Bcl-2 family members, pGBT9 plasmids containing *bcl-2* family members were cotransformed with fragments of human *beclin* (1 to 450, 262 to 450, and 1 to 708) fused to the GAL4 activation domain in pGAD424, and transformants were screened for LacZ activity.

Sequencing and analysis of human *beclin*. The partial nucleotide sequence of mouse *beclin* obtained from sequencing clone F1 was aligned with an overlapping clone GT197 isolated from human breast (32). Primers immediately upstream and downstream of the predicted open reading frame were used to amplify the coding sequence of human *beclin* from a normalized human infant brain cDNA library (37). The resulting PCR products from several independent reactions were cloned into pCRII and sequenced in both directions, using Sequenase (U.S. Biochemical) as well as automated sequencing. The resulting nucleotide sequence and deduced amino acid sequences were used to scan various data banks (GenBank, EMBL, SwissProt, and PIR) for homologous sequences, using the BLAST algorithms (2). The amino acid sequence was also analyzed by the PROSITE program to identify functional motifs and by the COILS program to identify coiled-coil regions (22).

Northern blot analysis. Human and mouse multiple tissue blots (Clontech) were hybridized with ^{32}P randomly labeled human or mouse *beclin* probes (nucleotides 1 to 485) as instructed by the manufacturer (Clontech). Equal loading [2 μg of poly(A) RNA] was confirmed by hybridization to a β-actin probe.

Production of recombinant viruses. The viruses SIN/*beclin*, SIN/*beclin*stop, SIN/*beclin*ΔBcl-2BD, SIN/*bcl-2*, and SIN/*bcl-2*stop were generated from viral cDNA clones as previously described (17). Briefly, 5′-capped transcripts were synthesized from cDNA clones linearized with *Pvu*I (for *beclin*-containing viruses) or *Xho*I (for *bcl-2*-containing viruses), transcribed in vitro with SP6 DNA-dependent RNA polymerase, and transfected into BHK cells by using Lipofectin according to the manufacturer's instructions. Twenty-four hours after transfection, virus particle-containing supernatants of transfected cell monolayers were collected, frozen in aliquots at 70°C, and used for all subsequent experiments. Titers of stock viruses were determined by plaque assay titration on BHK-21 cells.

Animal experiments. Ten-day-old litters of CD1 mice were inoculated intracerebrally into the right cerebral hemisphere with 1,000 PFU of each recombinant virus in 0.03 ml of Hanks' balanced salt solution. For mortality experiments, three to six separate litters were inoculated with each virus, and mortality was determined by daily observation of the mice for 3 weeks after infection. For virus titration and histopathology experiments, three to six mice per experimental group were sacrificed at days 1, 2, and 4 after inoculation. The right cerebral hemisphere was dissected and stored at −70°C, and freeze-thawed tissues were used to prepare 10% homogenates in Hanks' balanced salt solution for plaque assay titration. The left cerebral hemisphere was fixed by immersion in 3% paraformaldehyde.

Histopathology. Paraformaldehyde-fixed mouse brains were embedded in paraffin, and a series of 4-μm parasagittal sections were cut at the level of the olfactory bulb, extending caudally from the bulb to the cerebellum and medulla. For each brain, sequential sections were stained by hematoxylin and eosin to detect histopathology, in situ end labeling (ISEL) to detect apoptotic nuclei, in situ hybridization to detect Sindbis virus RNA, and immunoperoxidase to detect flag-Beclin protein expression. ISEL and in situ hybridization were performed by methods identical to those described previously for SIN/*bcl-2*-infected mouse brains (17). Immunoperoxidase staining to detect flag-Beclin protein expression in SIN/*beclin*-, SIN/*beclin*ΔBcl-2BD-, and SIN/*beclin*stop-infected mouse brains was performed by using the monoclonal anti-flag antibody M2 (5 μg/ml; VWR) and the avidin-biotin peroxidase method (Vectastain ABC kit; Vector Laboratories) according to the manufacturer's instructions.

The number of virus RNA-positive and ISEL-positive cells in each brain section was quantitated with Image-ProPlus software. To calculate the number of positive cells per brain section, nonoverlapping 0.25-mm^2 microscopic fields spanning the entire brain section were scanned with a 10× objective and constant settings for brightness, contrast, and threshold values for positive events. The number of positive events (i.e., RNA-positive cells or ISEL-positive cells) for each brain section was determined by adding the sum of all individual fields analyzed. The total number of positive events per brain section was divided by the total area of the brain section to yield the average number of RNA-positive or ISEL-positive cells per square millimeter of brain.

Sections of hippocampus and anterior cortex from an adult human were stained with 843, a polyclonal antibody against a human Beclin peptide corresponding to aa 1 to 15 (1:200 dilution; Eurogenetics, Seraing, Belgium), and human Beclin was detected by the avidin-biotin peroxidase method.

Plasmid transfections. Plasmids pSG5/*bcl-2* and pSG5/flag-*beclin* or pSG5/*bcl-2* and pSG5/flag-*beclin*ΔBcl-2BD (1 μg of each) were transiently transfected into COS7 cells by using Superfect (Qiagen) according to the manufacturer's instructions.

Protein detection. For immunofluorescence studies, COS7 cells were fixed 24 h after transfection with 100% ethanol. Expression of flag-Beclin and flag-mutant BeclinΔBcl-2BD mutant constructs was detected with an anti-flag epitope antibody (M2; 1:20; VWR) and fluorescein isothiocyanate (FITC)-conjugated horse anti-mouse immunoglobulin G. Bcl-2 expression was detected with a polyclonal rabbit anti-Bcl-2 antibody (1:100; Pharmingen) and rhodamine-conjugated goat anti-rabbit antibody. SERCA (endoplasmic reticulum Ca^{2+} ATPase) was detected with an anti-SERCA antibody (1:500; Research Design, Inc.). Western blot analysis to detect flag-Beclin expression in BHK cells infected with SIN/*beclin*, SIN/*beclin*stop, and SIN/*beclin*ΔBcl-2BD was performed with either antibody M2 (20 μg/ml) or anti-human Beclin peptide antibody 843 (1:200) and enhanced chemiluminescence detection as instructed by the manufacturer (Amersham).

FRET. Fluorescence resonance energy transfer (FRET) microscopy was performed as previously described on COS7 cells cotransfected with *bcl-2* and *beclin* expression vectors (9). The donor (FITC) filter set had the following parameters: excitation (ex) = 450 to 490 nm; dichroic mirror (dm) = 510 nm; emission (em) = 590 long pass. The acceptor (rhodamine) filter set had the following parameters: ex = 546 nm; dm = 580 nm, em = 590 long pass. Images obtained with these two filter sets were used to directly quantify the intensities of each fluorophore. The signal recorded from the FRET filter set (ex = 450 to 490 nm; dm = 580 nm; em = 590 nm long pass) is from energy that has transferred from FITC to rhodamine molecules. A mapping program described previously (9) was used to map fluorescent cells and to quantify the intensity within each cell. Quantitative analysis of these mapped images required solving three equations, one for each filter set, which accounted for the excitation and detection of both labels in all three filter sets as well as the concentrations of the donor and acceptor molecules and the probability of transfer. The measured quantities are expressed as follows, in which the first letter (uppercase) indicates the filter set (*A*, acceptor; *F*, FRET; *D*, donor) and the second letter (lowercase) indicates the labels present (*a*, acceptor alone; *f*, acceptor and donor; *d*, donor alone). A solution of the equation is $E = 1/[\mathrm{aconc}(RK + 1)]$, where $\mathrm{aconc} = (AdFf - FdAf)/[(AdFa/Aa) - Fd]$; $R = (DaFf/Fa - Df)/[\mathrm{aconc}((Fa/Aa) - FdDa/DdAa) - F = FdDf/Dd]$; and K is proportional to the product of the ratio of the quantum yield of the two labels and the ratio of the absolute detection efficiencies of the two labels.

Nucleotide sequence accession numbers. The GenBank accession numbers for human and mouse *beclin* are AF077301 and AF077302, respectively.

RESULTS

Identification of *beclin*, a novel gene on chromosome 17q21. Previously, we demonstrated that Bcl-2 inhibits Sindbis virus replication and prevents Sindbis virus-induced apoptosis in mouse neurons (17). To further understand the mechanisms by which Bcl-2 protects against Sindbis virus infection in neurons, we performed a yeast two-hybrid screen of an adult mouse brain library for complementary DNAs encoding proteins that bind to the cell death inhibitor Bcl-2. We constructed a bait plasmid (pGBT9/*bcl-2*) by fusing human *bcl-2* (lacking the C-terminal signal-anchor sequence to ensure translocation to the nucleus) to the GAL4 DNA-binding domain, which was cotransformed with an oligo(dT) and random hexamer-primed adult mouse brain cDNA fusion library in a GAL4 activation domain vector, pGAD10. Of 1 million transformants, one positive colony was identified by the 5-bromo-4-chloro-3-indolyl-β-D-galactopyranoside (X-Gal) filter assay. Sequencing

TABLE 1. Summary of yeast two-hybrid assay results

GAL4 activation domain plasmid[b]	β-Galactosidase reaction with GAL4 binding domain construct[a]						
	Empty	Bcl-2	Bcl-x_L	Bcl-x_S	Bax	Lamin	p53
Empty	−	−	−	+	−	−	−
F1							
1–2563	−	+	+	ND	−	−	−
1–1855	−	−	−	ND	−	−	−
1856–2563 (*Mus* Beclin 1–708)	−	+	+	ND	−	−	−
Human Beclin							
1–708	−	+	+	ND	−	−	−
Beclin 1–450	−	+	+	ND	−	−	−
Beclin 1–258	−	−	−	ND	−	−	−
Beclin 262–450	−	+	+	ND	−	−	−
Beclin 451–708	−	−	−	ND	−	−	−
Beclin 1–1353	−	−	−	ND	−	−	−

[a] +, positive reaction within 15 min; −, lack of positive reaction at 24 h; ND, not determined.
[b] Nucleotide positions of genes fused to the plasmid.

analysis of the cDNA plasmid rescued from this colony (F1) revealed a termination codon 42 bp downstream from the GAL4 activation domain, several predicted short open reading frames between nucleotides 124 and 1843 and a longer predicted open reading frame (with a good Kozak consensus sequence and multiple stop codons upstream) spanning from nucleotide 1855 to the 3′ end of the insert. Thus, either the 14-aa fusion protein was interacting with Bcl-2 or one of the downstream open reading frames encoded a protein that contains its own activation domain and interacts with Bcl-2. To identify the Bcl-2-interacting region of F1, we fused nucleotides 1 to 1854 and 1855 to 2500 to the GAL4 activation domain in pGAD424 and tested for interactions with Bcl-2. Nucleotides 1855 to 2500, but not 1 to 1854, encoded a protein that interacts with Bcl-2 fused to the GAL4 DNA-binding domain (Table 1) but not with control GAL4 DNA-binding domain plasmids containing p53, lamin (Table 1), or Sindbis virus glycoproteins (data not shown).

A database search revealed that the nucleotide sequence of F1 (1855 to 2500) overlapped with sequences of several clones isolated from a normalized infant human brain cDNA library in the Merck EST (epitope tag sequence) database as well as clones from human breast (GT197) (32) and human fibroblast (B32) cells (8). These clones contain only partial open reading frames of a novel gene that encodes a protein with coiled coils. As explained above, we assigned the name *beclin* to this gene because of the interaction of its encoded protein with Bcl-2 and the predicted coiled-coil structure of its encoded protein. Clones GT197 and B32 were both isolated in the generation of transcription maps of the breast cancer susceptibility locus on chromosome 17q21 and are mapped to a region located approximately 100 kb centromeric to the gene *BRCA1*. They lie within a 400-kb minimal deletion unit mapped by Tangir et al. in sporadic epithelial ovarian cancers (38).

We aligned the overlapping partial clones in GenBank with our mouse *beclin* sequence to obtain a predicted sequence of the full-length open reading frame of human *beclin* and isolated human *beclin* from a normalized human infant brain cDNA library (37). Human *beclin* is predicted to encode a novel 450-aa, 60-kDa protein containing a coiled-coil region with 25 to 28% homology with myosin-like proteins (Fig. 1). It shares 93% identity at the nucleotide level and 98% identity at the amino acid level with the mouse *beclin* sequence identified in the yeast two-hybrid screen. Human Beclin is also homologous with the *Caenorhabditis elegans* T19E7.3 gene product (GenBank accession no. U42843) and the *S. cerevisiae* gene product Lph7p (GenBank accession no. U43503) (38 and 37% identical over 145 and 137 residues, respectively), indicating a high degree of evolutionary conservation. PROSITE analysis of human Beclin identified several potential glycosylation, phosphorylation, and myristoylation sites but no other functional sequence motifs.

Ubiquitous expression of *beclin* mRNA in mouse and human tissues. To examine the tissue-specific pattern of *beclin* expression, we hybridized mouse and human multiple-tissue Northern blots with a *beclin*-specific probe. RNA blot analysis revealed that expression of *beclin* mRNA is widespread in both mouse and human adult tissue (Fig. 2A). A *beclin*-specific probe hybridized to a 2.2-kb transcript present at highest levels in human skeletal muscle but at detectable levels in all tissues examined. The size of this transcript is approximately the same as that observed previously for clones GT197 and B32 (8, 32). In some tissues, additional 1.7- and 1.4-kb transcripts were observed, suggesting the presence of alternatively spliced transcripts.

Beclin is expressed in human neurons. To examine whether Beclin protein is expressed in neurons (the primary CNS target cell type for Sindbis virus infection), we performed immunoperoxidase staining of adult human brain sections. We used rabbit immune serum 843, generated against a human Beclin peptide corresponding to aa 1 to 15. 843 reacts with a 61-kDa protein in lysates prepared from BHK cells after infection with a recombinant Sindbis virus containing a flag epitope-tagged human *beclin* insert (SIN/*beclin*) (Fig. 3B). This protein migrates identically to the major band detected with an anti-flag epitope antibody in SIN/*beclin*-infected BHK cell lysates (Fig. 3A) and to in vitro translated flag-Beclin (data not shown). Immunoperoxidase staining of human brain sections from the hippocampus and frontal cortex revealed Beclin immunoreactivity in many neurons throughout these regions as well as in some glial cells. In neurons, Beclin demonstrated a granular, punctate pattern of staining that was found almost exclusively in the region of the perikaryon (Fig. 2B). Beclin immunoreac-

```
1    M E G S K T S N N S T M Q V S F V C Q R C S Q P L K L D T S
31   F K I L D R V T I Q E L T A P L L T T A Q A K P G E T Q E E
61   E T N S G E E P F I E T P R Q D G V S R R F I P P A R M M S
91   T E S A N S F T L I G E A S D G G T M E N L S R R L K V T G
121  D L F D I M S G Q T D V D H P L C E E C T D T L L D Q L D T
151  Q L N V T E N E C Q N Y K R C L E I L E Q M N E D D S E Q L
181  Q M E L K E L A L E E E R L I Q E L E D V E K N R K I V A E
211  N L E K V Q A E A E R L D Q E E A Q Y Q R E Y S E F K R Q Q
241  L E L D D E L K S V E N Q M R Y A Q T Q L D K L K K T N V F
271  N A T F H I W H S G Q F G T I N N F R L G R L P S V P V E W
301  N E I N A A W G Q T V L L L H A L A N K M G L K F Q R Y R L
331  V P Y G N H S Y L E S L T D K S K E L P L Y C S G G L R F F
361  W D N K F D H A M V A F L D C V Q Q F K E E V E K G E T R F
391  C L P Y R M D V E K G K I E D T G G S G G S Y S I K T Q F N
421  S E E Q W T K A L K F M L T N L K W G L A W V S S Q F Y N K
```

FIG. 1. Deduced amino acid sequence of human Beclin. The boxed area represents the Bcl-2-binding domain of human Beclin (Table 1), and the underlined area corresponds to the region that is predicted to have a coiled-coil conformation.

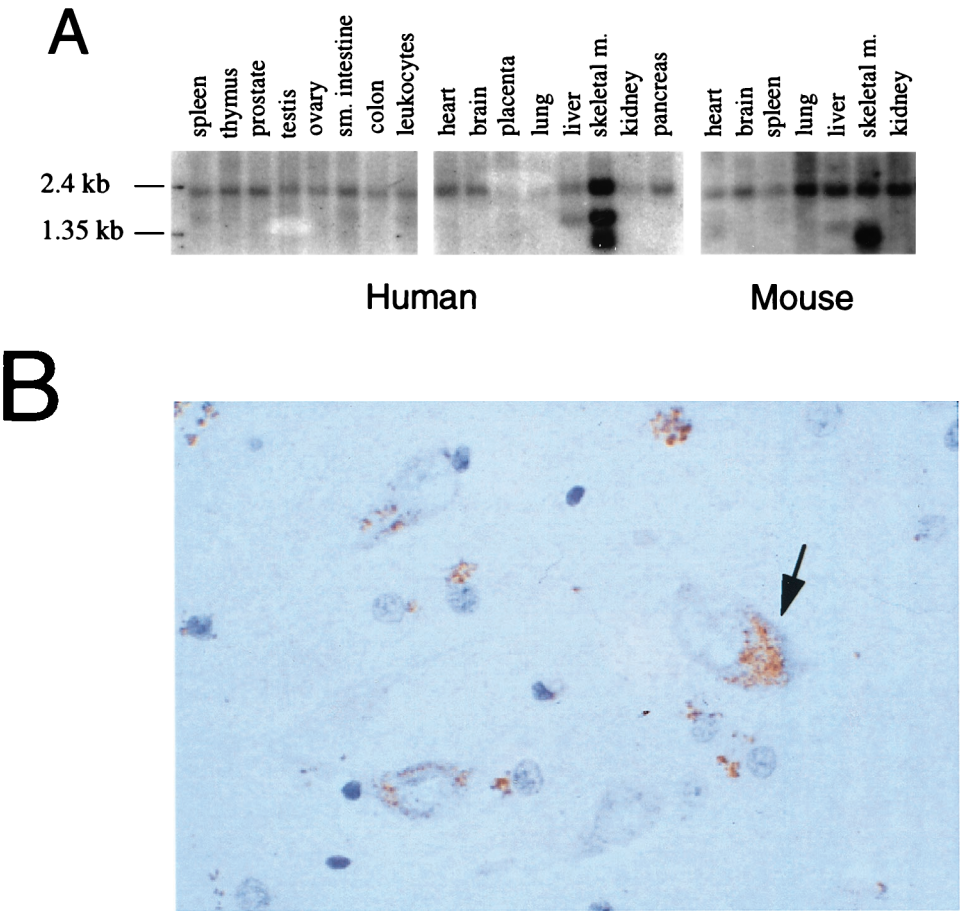

FIG. 2. Beclin mRNA and protein expression. (A) Northern blot analysis of *beclin* mRNA expression in human and mouse tissues. sm., small; m., muscle. (B) Immunoperoxidase staining of an adult human hippocampus section with a polyclonal antibody against a human Beclin peptide. The arrow marks a Beclin-positive neuron. Magnification, ×450.

tivity was also observed in the media of blood vessels, in the ependymal cells, and in the choroid plexus. No staining was observed in human brains stained with rabbit preimmune serum 843 (data not shown).

Interaction of Beclin and Bcl-2. We performed additional yeast two-hybrid studies to confirm that human *beclin*, like mouse *beclin*, encodes a protein that interacts with human Bcl-2 and to further define the Bcl-2-interacting region of human Beclin (Table 1). We found that the region of human Beclin that corresponds to the mouse gene product isolated in the yeast two-hybrid screen (aa 1 to 236) also interacts with Bcl-2. Further deletion mutation analysis revealed that aa 88 to 150 of Beclin were sufficient to mediate an interaction with Bcl-2. Interestingly, the coding sequence for this region of Beclin is deleted in some human infant brain cDNA clones in the Merck EST database, suggesting that Beclin exists in at least two forms, including one that contains a Bcl-2-binding domain and one that lacks this domain. Full length-Beclin does not interact with Bcl-2 in the yeast two-hybrid system. As noted below, when expressed in transient transfection assays, flag-tagged full-length human Beclin displays a punctate immunoreactivity pattern suggestive of association with intracellular organelles and is associated with the insoluble fraction after cell lysis. In contrast, a flag-tagged truncated Beclin (aa 1 to 236) (corresponding to the region isolated in the yeast two-hybrid screen) displays a diffuse cytoplasmic staining pattern and is soluble after cell lysis. These differences between full-length and truncated Beclin are thought to account for differences in ability to translocate to yeast nuclei and interact with Bcl-2 in the yeast two-hybrid assay.

To directly examine whether full-length human Beclin and Bcl-2 interact in mammalian cells, we performed FRET studies of COS7 cells cotransfected with Bcl-2 and flag epitope-tagged Beclin. Beclin is predicted to be a coiled-coil protein that may be associated with the cytoskeleton, and it partitions with the insoluble fraction following cell lysis. For this technical reason, biochemical analyses of in vivo interactions between Bcl-2 and Beclin cannot be performed. FRET is a fluorescence technique that can be used as a spectroscopic ruler to study and quantify the interactions of cellular components with each other (reviewed in references 6, 12, and 35). In FRET, a fluorophore (donor) in an excited state may transfer its excitation energy to a neighboring chromophore (acceptor) nonradiatively through dipole-dipole interactions. The efficiency of this process varies as the inverse of the sixth power of the distance separating the donor and acceptor chromophores and, in practice, requires the distance between the donor and acceptor fluorophores to be short (usually less than 50 Å). The dependence of the energy transfer efficiency on the donor-acceptor separation provides the basis for the utility of this phenomenon in the study of cell component interactions. FRET has been used by a number of investigators to examine interactions of cellular

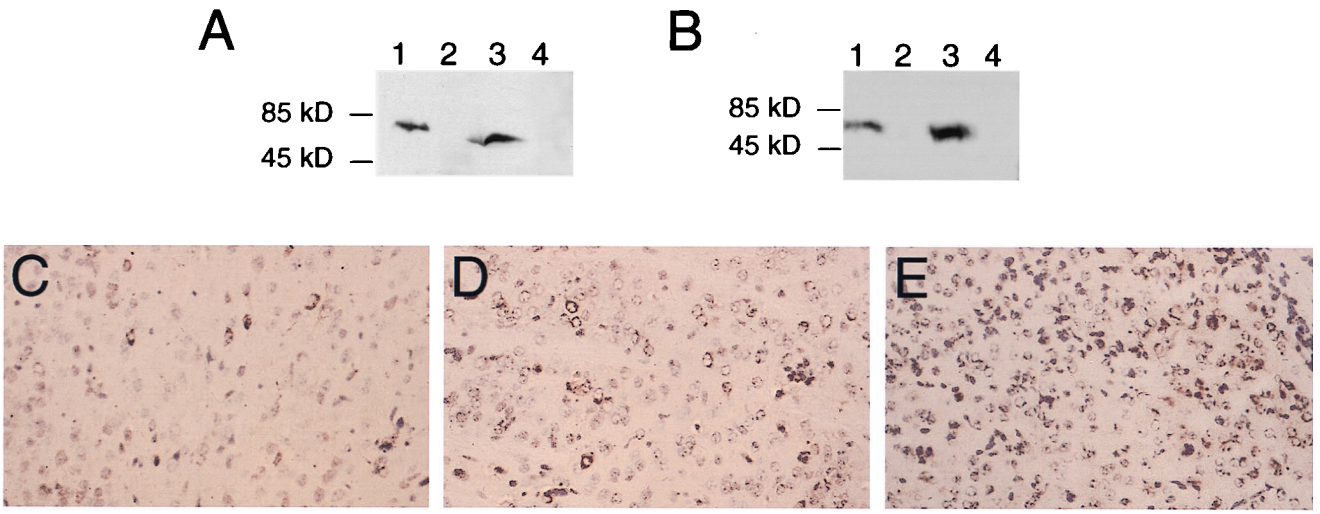

FIG. 3. Expression of flag-Beclin protein constructs by the virus vectors SIN/*beclin*, SIN/*beclin*stop, and SIN/*beclin*ΔBcl-2BD. (A and B) Western blot analyses of virus-infected BHK cell lysates with either anti-flag epitope antibody M2 (A) or polyclonal rabbit anti-Beclin antiserum (B). Lane 1, SIN/*beclin*; lane 2, SIN/*beclin*stop; lane 3, SIN/*beclin*ΔBcl-2BD; lane 4, empty Sindbis virus vector. (C to E) Immunoperoxidase staining using anti-flag epitope antibody M2 of mouse brains 2 days after infection with SIN/*beclin* (C), SIN/*beclin*stop (D), or SIN/*beclin*ΔBcl-2BD (E). Magnification, ×111.

constituents (reviewed in 6, 12, and 35) such as endosomal fusion events, ligand-dependent growth factor receptor aggregations, interactions of viral and cellular proteins with regulators of apoptosis (20), and interactions of cellular cytoskeletal components (33).

Prior to measuring FRET, we first confirmed the colocalization of full-length Bcl-2 and Beclin in transfected COS7 cells, using confocal laser microscopy (Fig. 4). Bcl-2 is known to associate with the outer mitochondrial membrane, endoplasmic reticulum, and perinuclear membranes, and it displays a punctate pattern of cytoplasmic immunoreactivity (reviewed in reference 28). We found that flag-Beclin invariably displayed a pattern of immunoreactivity identical to that of Bcl-2 in all cotransfected COS7 cells examined by confocal laser microscopic analysis (Fig. 4A to C). Furthermore, we found that deletion of the putative Bcl-2-binding domain from Beclin did not alter its pattern of immunoreactivity; flag-BeclinΔBcl-2BD appeared to have a pattern of staining similar to that of full-length Beclin, and like full-length Beclin, it colocalized with Bcl-2 in cotransfected cells (Fig. 4D to F). This granular pattern of Beclin immunoreactivity in the perinuclear region is similar to that observed for endogenous Beclin in human neurons (compare Fig. 2B, 4A, and 4D).

After confirming the colocalization of Bcl-2 and Beclin and of Bcl-2 and BeclinΔBcl-2BD, we used FRET analysis to determine whether Bcl-2 and Beclin physically interact. We compared in transfected COS7 cells the amounts of FRET between Bcl-2 and full-length Beclin, Bcl-2 and BeclinΔBcl-2BD, and Bcl-2 and a control protein, SERCA. Quantitative analysis of microscopic images (following corrections for cross-talk between filter sets and donor and acceptor concentrations) showed significantly more FRET in cells with labeled full-length Beclin and Bcl-2 ($E_{\text{Beclin-Bcl-2}} = 0.000578 \pm 0.000262$; mean ± standard error of the mean [SEM], $n = 410$) than in cells with labeled BeclinΔBcl-2BD and Bcl-2 ($E_{\text{BeclinΔBcl-2BD-Bcl-2}} = 0.000189 \pm 0.000151$; $n = 2,946$) ($P = 0.0068$, t test) or in cells with labeled SERCA and Bcl-2 ($E_{\text{SERCA-Bcl-2}} = 0.0000639 \pm 0.0000390$; $n = 775$) ($P = 0.0021$, t test). These quantitative analyses indicate that Beclin and Bcl-2 exhibit FRET and provide evidence of an interaction between these two proteins in mammalian cells. Furthermore, deletion of the Bcl-2-binding domain of Beclin mapped in yeast two-hybrid studies does not alter the spatial orientation of transfected Beclin, but it does significantly decrease FRET. This observation suggests that the FRET observed between full-length Beclin and Bcl-2 reflects a specific association of these proteins in vivo, rather than an artifact secondary to overexpression.

Selective interaction of Beclin with death repressor members of the Bcl-2 family. To investigate whether Beclin interacts with other Bcl-2 family members that positively or negatively regulate apoptosis, we fused *bax*, *bcl-x*$_S$, and *bcl-x*$_L$ into the GAL4 binding domain vector and tested for interactions with Beclin in the yeast two-hybrid system (Table 1). The Bcl-x$_S$ GAL4 binding domain construct activated transcription by itself and therefore could not be tested for interactions with Beclin. The same region of Beclin (aa 88 to 150) that interacted with Bcl-2 also interacted with Bcl-x$_L$, a related Bcl-2 family member that inhibits apoptosis (4). In contrast, Beclin did not react with Bax, a family member that promotes apoptosis (27). This pattern of interaction, i.e., with Bcl-2 and Bcl-x$_L$, but not Bax, is identical to that observed for all previously identified Bcl-2-interacting proteins outside the Bcl-2 family (reviewed in reference 30).

Mutations in Bcl-2 and Bcl-x$_L$ that block death repressor activity also block binding to Beclin. Cheng et al. have shown that Bcl-2 and Bcl-x$_L$ overexpression can delay Sindbis virus-induced death of BHK cells (5). To evaluate whether Bcl-2–Beclin and Bcl-x$_L$–Beclin interactions may be related to this ability of Bcl-2 and Bcl-x$_L$ to inhibit Sindbis virus-induced apoptosis, we constructed pGBT9 vectors containing *bcl-2* and *bcl-x*$_L$ constructs with mutations in the conserved BH1 domain that are known to block death repressor activity. A Gly-Ala mutation at amino acid position 145 of Bcl-2 completely abrogates Bcl-2 death repressor activity in interleukin-3 deprivation-, γ-irradiation- and glucocorticoid-induced apoptosis (42) and also blocks Bcl-2 binding to Beclin in the yeast two-hybrid system (Table 2). Similarly, substitution of aa 136 to 138 of Bcl-x$_L$ (VNX→AIL) completely abolishes death repressor activity in Sindbis virus-induced apoptosis (5) and also blocks Bcl-x$_L$ binding to Beclin (Table 2). These mutations in Bcl-2

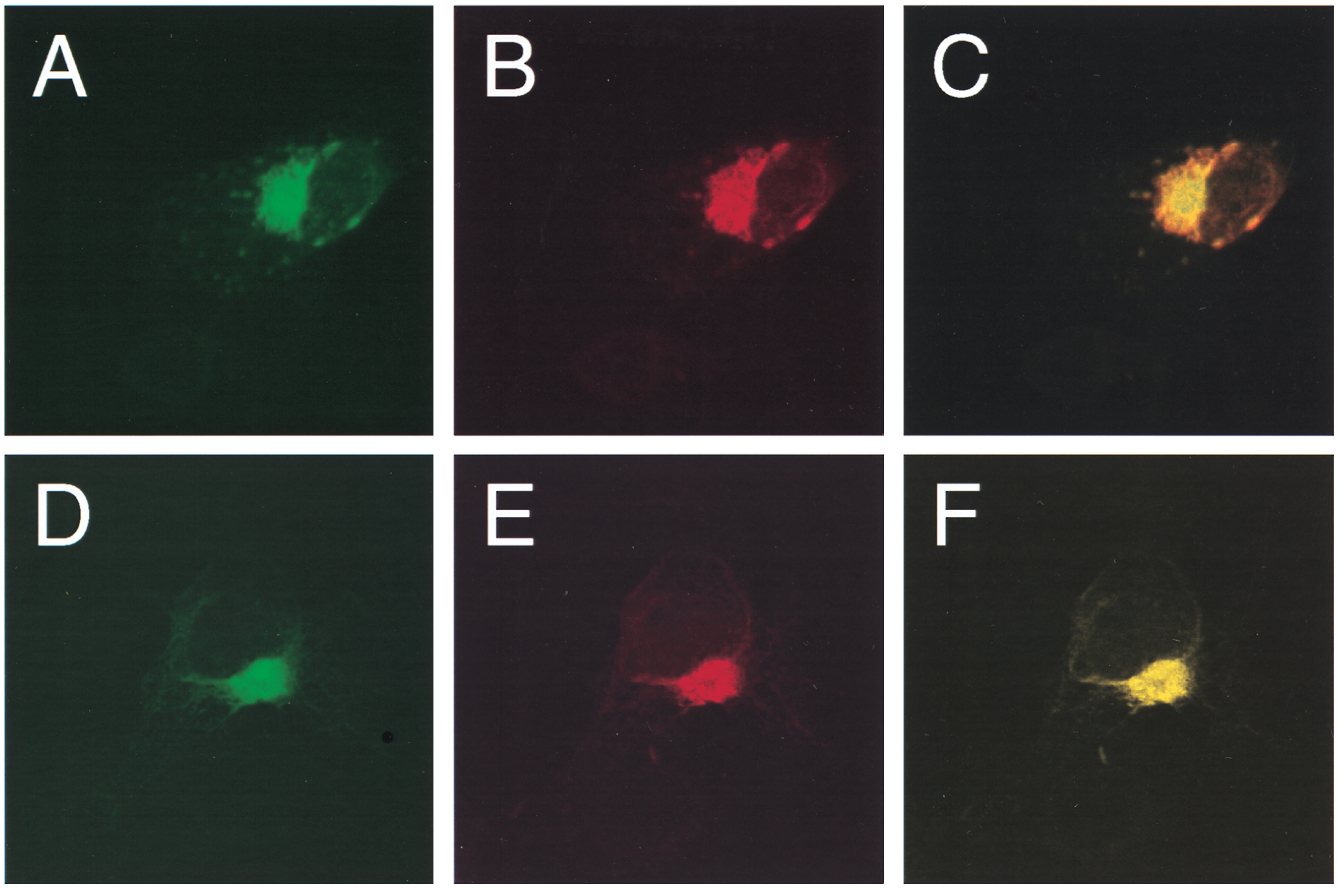

FIG. 4. Confocal laser scanning microscopy of COS7 cells expressing Bcl-2 and Beclin. (A and B) Cell cotransfected with pSG5/*bcl-2* and pSG5/flag-*beclin* and stained with anti-flag epitope (A) and anti-human Bcl-2 (B) antibodies. (D and E) Cell cotransfected with pSG5/*bcl-2* and pSG5/flag-*beclin*DBcl-2BD and stained with anti-flag epitope (D) and anti-human Bcl-2 (E) antibodies. (C and F) Computerized overlays of panels A and B (C) and panels D and E (F); yellow color corresponds to overlap of FITC and rhodamine staining. Confocal slides were 1 μm thick.

(G→A145) and Bcl-x_L (VNW→AIL) did not alter the level of Bcl-2 or Bcl-x_L expression in yeast cells (data not shown), indicating that the lack of interaction could not be attributed to effects of the mutations on protein expression in yeast. These data therefore demonstrate that mutations that block the antideath activity of Bcl-2 and Bcl-x_L also block binding to Beclin.

Beclin protects mice against fatal encephalitis caused by the neurovirulent TE12 strain of Sindbis virus. After identifying Beclin as a novel Bcl-2-interacting protein that is expressed in neurons, we were interested in studying its effects on Sindbis virus infection. To directly evaluate the role of Beclin and its potential interactions with Bcl-2-like proteins in modulating Sindbis virus pathogenesis, we compared the natural histories of mice infected with recombinant chimeric viruses that express either wild-type human Beclin (SIN/*beclin*), human Beclin lacking the putative Bcl-2-binding domain (SIN/*beclin*ΔBcl-2BD), or human Beclin containing a premature stop codon at nucleotide position 270 (SIN/*beclin*stop).

To construct these viruses, we used a strategy identical to that previously described for Sindbis virus chimeras that express human Bcl-2 (17), with the exception that we used a more neurovirulent background strain of Sindbis virus, dsTE12. We chose dsTE12 rather than the previously used less virulent strain ds633 because of the possibility that the larger size of the human *beclin* open reading frame insert would have an attenuating effect on Sindbis virus neurovirulence. Whereas ds633 is neurovirulent only in neonatal mice, dsTE12 is also neurovirulent in older mice (40). ds633 and dsTE12 differ at one amino acid position in the E2 envelope glycoprotein (Gln-55 in ds633; His-55 in dsTE12) and two amino acid positions in the E1 glycoprotein (Val-72 and Gly-313 in ds633; Ala-72 and Asp-313 in dsTE12). Previous studies with recombinant viruses have mapped the amino acid residue responsible for neurovirulence in older mice to position 55 in E2 (40, 41).

We confirmed that SIN/*beclin* and SIN/*beclin*ΔBcl-2BD expressed proteins of the predicted molecular weights by performing Western blot analyses of infected BHK cell lysates with both an anti-flag epitope monoclonal antibody and a polyclonal anti-human Beclin peptide antibody (Fig. 3A and B). SIN/*beclin* expressed a 61-kDa protein and SIN/*beclin*ΔBcl-2BD expressed a 52-kDa protein reactive with both anti-flag

TABLE 2. Effect of BH1 domain mutations on the ability of Bcl-2 and Bcl-x_L to bind to Beclin in the yeast two-hybrid assay

Construct[a]	Conserved BH1 domain	Inhibition of apoptosis (reference)	Beclin binding
WT Bcl-2	ELFRDGVNWGRIVAFFEFGG	+	+
WT Bcl-x_L	ELFRDGVNWGRIVAFFSFGG	+	+
MT Bcl-2	---------A----------	− (42)	−
MT Bcl-x_L	------AIL----------	− (5)	−

[a] WT, wild-type; MT, mutant.

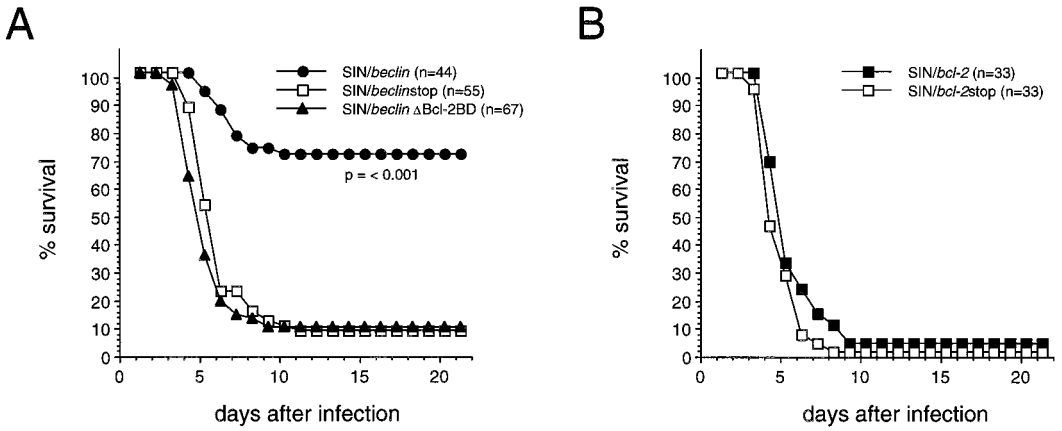

FIG. 5. Effects of Beclin and Bcl-2 on the survival of mice infected with Sindbis virus strain TE12. (A) Survival curve of mice infected with SIN/*beclin*, SIN/*beclin*stop, and SIN/*beclin*ΔBcl-2BD. Data represent combined survival probabilities for four to six independent litters. (B) Survival curve of mice infected with SIN/*bcl-2* and SIN/*bcl-2*stop. Data represent combined survival probabilities for three independent litters.

epitope and anti-Beclin antibodies. We also confirmed that human flag-Beclin and flag-BeclinΔBcl-2BD were expressed in virally infected neurons by performing immunoperoxidase staining of mouse brains at days 1, 2, and 4 after infection (representative photomicrographs shown in Fig. 3C and E). Although we did not detect any flag-Beclin protein expression by Western blot analysis of BHK cell lysates infected with SIN/*beclin*stop, flag immunoreactivity was also observed in mouse brains infected with SIN/*beclin*stop (Fig. 3D). No flag immunoreactivity was seen in control mouse brains infected with the dsTE12 vector alone (data not shown). Fewer flag-immunoreactive cells were observed in SIN/*beclin*-infected than in SIN/*beclin*ΔBcl-2- and SIN/*beclin*stop-infected mouse brains.

We compared the survival of 10-day-old litters of CD1 mice infected intracerebrally with 1,000 PFU of SIN/*beclin*, SIN/*beclin*ΔBcl-2BD, and SIN/*beclin*stop (Fig. 5A). The survival of mice infected with SIN/*beclin* was 71%, compared with only 9 and 7% after infection with SIN/*beclin*ΔBcl-2BD and SIN/*beclin*stop. The differences in survival between groups infected with SIN/*beclin* versus SIN/*beclin*ΔBcl-2BD and SIN/*beclin* versus SIN/*beclin*stop were highly significant ($P < 0.001$; life-table analysis). Thus, full-length Beclin overexpression in virally infected neural cells results in marked protection against fatal Sindbis virus encephalitis. Furthermore, the high mortality after infection with a virus expressing a mutant form of Beclin lacking the Bcl-2-binding domain suggests that binding to Bcl-2 or Bcl-2-like proteins is important for the protective effects of Beclin on survival in Sindbis virus encephalitis.

Bcl-2 does not protect against fatal encephalitis caused by TE12. Previously, we showed that Bcl-2, expressed in the ds633 Sindbis virus vector, protected neonatal mice against fatal Sindbis virus infection (17). However, in in vitro studies in AT3/bcl-2 cells, the TE12 strain overcomes protection conferred by Bcl-2 (41). To directly compare the abilities of Beclin and Bcl-2 to protect against encephalitis by TE12 in 10-day-old mice, we cloned human *bcl-2* and human *bcl-2* containing a premature stop codon after nucleotide position 118 into the dsTE12 vector to generate the constructs SIN/*bcl-2* and SIN/*bcl-2*stop. Unlike SIN/*beclin* versus SIN/*beclin*stop (Fig. 5A), there was no difference in the survival of mice infected with SIN/*bcl-2* versus SIN/*bcl-2*stop (Fig. 5B). Together with previous results (17), these data demonstrate that Bcl-2 can protect against fatal encephalitis caused by a strain of Sindbis virus containing a wild-type glutamine at position E2 position 55 but not by a more neurovirulent strain of Sindbis virus containing a histidine mutation at E2 position 55 (E2-55 histidine mutation).

Beclin reduces Sindbis virus replication in mouse brain. To examine whether Beclin overexpression affects Sindbis virus replication, we measured viral titers of mouse brain homogenates and performed in situ hybridization of mouse brain sections to detect message-sense viral RNA. Mean viral titers were reduced 5-fold at day 1 and 50-fold at days 2 and 4 after infection in brains of mice infected with SIN/*beclin* compared to the brains of mice infected with SIN/*beclin*stop or SIN/*beclin*Δbcl-2BD (Fig. 6). Computerized quantitative image analysis of virus RNA positive cells in infected mouse brains showed an inhibitory effect of Beclin on viral replication that was similar to, but had a temporal pattern somewhat different from, that observed by measurement of viral titers (Fig. 7). The mean number of virus RNA-positive cells was significantly lower in brains infected with SIN/*beclin* than in brains infected with SIN/*beclin*stop at day 4 after infection (100 ± 36 versus 494 ± 55; $P = 0.004$, *t* test) but was equivalent at day 2 after infection (575 ± 272 versus 507 ± 216; $P = 0.854$, *t* test). The reduction of viral titers but not of virus RNA-positive cells in mouse

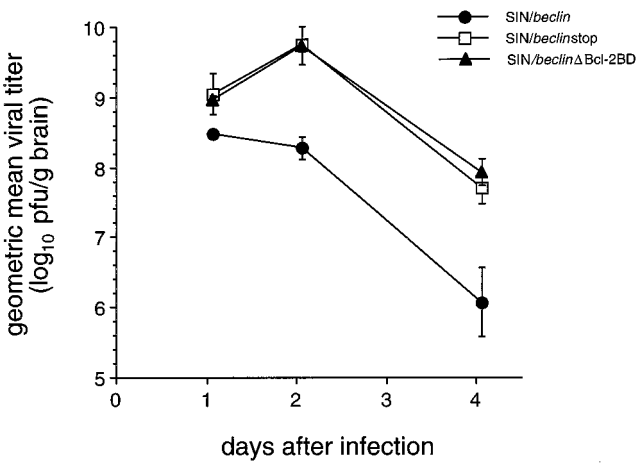

FIG. 6. Viral growth of SIN/*beclin*, SIN/*beclin*stop, and SIN/*beclin*ΔBcl-2BD in mouse brain. Each data point represents geometric mean viral titer ± SEM of three to six mouse brains.

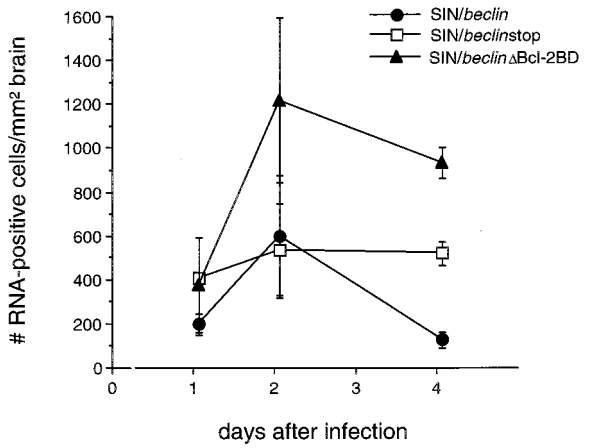

FIG. 7. Viral RNA-positive cells in mouse brains infected with SIN/*beclin*, SIN/*beclin*stop, and SIN/*beclin*ΔBcl-2BD. Each data point represents the mean ± SEM number of Sindbis virus message-sense RNA-positive cells per square millimeter of brain for three to six mouse brains.

brains 2 days after infection with SIN/*beclin* suggests a possible inhibitory effect of Beclin on posttranscriptional stages of viral replication. In addition, the viral titers of SIN/*beclin*ΔBcl-2BD-infected mouse brains did not differ significantly from titers of SIN/*beclin*stop-infected mouse brains, but the number of virus RNA-positive cells was higher at days 2 and 4 in SIN/*beclin*ΔBcl-2BD-infected than in SIN/*beclin*stop-infected mouse brains. This difference was significant at day 4 (905 ± 72 versus 494 ± 55; $P = 0.01$, *t* test) but not at day 2 (1,190 ± 375 versus 507 ± 216; $P = 0.190$, *t* test) after infection.

The anatomic distribution of RNA-positive cells did not differ among the different virus-infected groups; viral RNA-positive cells were found in clusters scattered throughout the brain, most commonly in the subventricular zone, posterior neocortex, colliculus, hippocampus, striatum, and olfactory bulb. However, the number of cells seen within a given cluster was usually lowest in SIN/*beclin*-infected mouse brains and greatest in SIN/*beclin*ΔBcl-2BD-infected mouse brains (see representative photomicrographs in Fig. 9).

Beclin reduces Sindbis virus-induced cell death in mouse brain. To examine whether CNS Beclin overexpression reduces apoptotic cell death, we quantitated the number of apoptotic nuclei in the brains of mice infected with the chimeric viruses SIN/*beclin*, SIN/*beclin*stop, and SIN/*beclin*ΔBcl-2BD (Fig. 8). Within each mouse brain, almost all apoptotic nuclei were found in regions that had detectable viral RNA by in situ hybridization (Fig. 9) and in regions that had histopathologic evidence of neuronal death. A close association was observed between the mean numbers of apoptotic nuclei at each time point among the three different virus treatment groups and the mean numbers of virus RNA-positive cells (compare results in Fig. 7 and 8). In mouse brains infected with SIN/*beclin* and SIN/*beclin*stop, little cell death was seen at days 1 and 2 after infection, and the number of apoptotic cells per square millimeter of brain did not differ between these groups. More apoptotic nuclei were present at day 2 after infection in the brains of mice infected with SIN/*beclin*ΔBcl-2BD (604 ± 211) than in the brains of mice infected with SIN/*beclin* (133 ± 90) or SIN/*beclin*stop (91 ± 52); this difference was nearly statistically significant ($P = 0.078$, analysis of variance). At day 4 after infection, the mean number of apoptotic cells per square millimeter of brain was markedly increased in SIN/*beclin*stop (1,490 ± 29) and SIN/*beclin*ΔBcl-2BD (1,044 ± 430) versus SIN/*beclin*-infected mouse brains (101 ± 10; $P = 0.001$, analysis of variance). These data demonstrate that Beclin overexpression decreases apoptotic death in mouse brains infected with the TE12 strain of Sindbis virus.

DISCUSSION

In this study, we describe the identification of a novel coiled-coil 60-kDa protein, Beclin, which interacts with the cell death regulator Bcl-2. We demonstrate that Beclin overexpression in virally infected neurons in vivo results in substantial protection against Sindbis virus-induced disease. Mice infected with recombinant Sindbis viruses that express wild-type Beclin have less neural cell apoptosis, decreased viral replication, and a significant lower mortality rate than mice infected with recombinant viruses that express Beclin deletion mutants. Furthermore, the Bcl-2-binding domain of Beclin is required for the antiviral, antiapoptotic, and survival-promoting effects of Beclin on CNS Sindbis virus infection. These findings suggest that Beclin, via interactions with Bcl-2-like molecules, can function in vivo in the CNS as an antiviral host defense molecule.

Our conclusion that the protective, antiviral effects of Beclin are mediated through interactions with Bcl-2 (or Bcl-2-like molecules that bind to same region of Beclin as Bcl-2) is supported by data obtained with a chimeric Sindbis virus expressing Beclin lacking aa 88 to 151. Amino acids 88 to 150 of Beclin are sufficient to mediate an interaction with Bcl-2 and Bcl-x_L in the yeast two-hybrid assay, and deletion of these amino acids from full-length Beclin significantly decreases the strength of the Beclin-Bcl-2 interaction in mammalian cells. The Sindbis virus construct expressing Beclin lacking aa 88 to 150 (SIN/*beclin*ΔBcl-2BD) replicated to as high levels in mouse brain, resulted in as much apoptotic neural cell death, and resulted in the same mortality in mice as a control recombinant virus which expressed a 90-aa truncated Beclin protein (SIN/*beclin*-stop). The lack of protective activity of BeclinΔBcl-2BD compared to full-length Beclin cannot be attributed to lower levels of BeclinΔBcl-2BD expression after infection with SIN/*beclin*ΔBcl-2BD. The levels of flag-BeclinΔBcl-2BD were equal to or greater than levels of flag-Beclin detected by immunoblot analysis of lysates from BHK cells infected with SIN/*beclin* and SIN/*beclin*ΔBcl-2BD, respectively. In addition, SIN/*beclin*ΔBcl-2BD-infected mouse brains had more flag-immunoreactive cells than mouse brains infected with SIN/*beclin*.

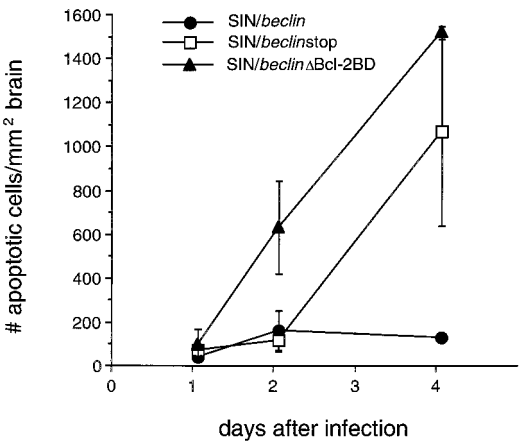

FIG. 8. Apoptotic nuclei in mouse brains infected with SIN/*beclin*, SIN/*beclin*stop, and SIN/*beclin*ΔBcl-2BD. Each data point represents the mean ± SEM number of ISEL-positive nuclei per square millimeter of brain for three to six mouse brains.

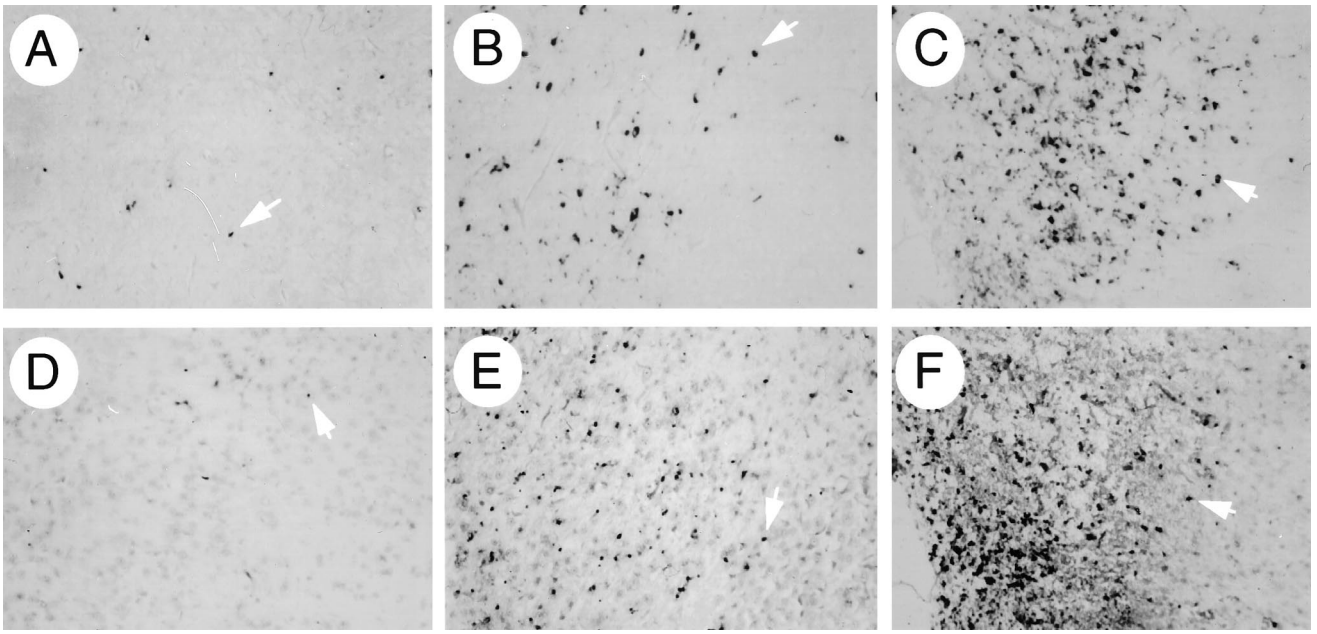

FIG. 9. Representative photomicrographs of fields used for computerized quantitative image analysis of viral RNA (A to C)- and ISEL (D to F)-positive cells in mouse brains infected with SIN/*beclin* (A and D), SIN/*beclin*stop (B and E), and SIN/*beclin*ΔBcl-2BD (C and F) in Fig. 7 and 8, respectively. All photomicrographs are from the colliculus region of brain sections 4 days after infection and correspond to the images observed at a magnification of ×10. Arrowheads denote representative cells that were scored as positive by the Image-ProPlus software program.

Thus, the lack of protective activity of BeclinΔBcl-2 is most consistent with the hypothesis that the antiviral effects of Beclin are mediated through interactions with Bcl-2-like proteins.

Some of the data in the present study suggest that the virus SIN/*beclin*ΔBcl-2BD may be more neurovirulent than the virus SIN/*beclin*stop. Mice infected with SIN/*beclin*ΔBcl-2BD had more virus RNA-positive cells in their brains at days 2 and 4 after infection than mice infected with SIN/*beclin*stop. Corresponding to the more rapid spread of infection, more cell death was seen earlier on after infection in the brains of mice infected with SIN/*beclin*ΔBcl-2BD compared to SIN/*beclin*stop. Although the overall mortality rates of mice infected with SIN/*beclin*ΔBcl-2BD versus SIN/*beclin* stop did not differ, but the mean day of death was slightly lower in mice infected with SIN/*beclin*ΔBcl-2BD versus SIN/*beclin*stop. These observations raise the possibility that Beclin lacking the Bcl-2-binding domain functions as a dominant negative mutant. As a corollary, the naturally occurring Beclin isoform found in brain that lacks the Bcl-2-binding domain may serve as a death-promoting molecule.

Beclin may exert antiviral effects via interactions with either Bcl-2, Bcl-x_L, or yet unidentified Bcl-2 family members. In yeast two-hybrid assays, we found that the same region of Beclin interacted with Bcl-2 and Bcl-x_L and that loss-of-function mutations in the conserved BH1 domains of both Bcl-2 and Bcl-x_L blocked binding to Beclin. While both Bcl-2 and Bcl-x_L are important regulators of apoptosis in neurons (reviewed in reference 23), we have found that Bcl-2, but not Bcl-x_L, protects mice against fatal encephalitis and delays Sindbis virus-induced death of cultured rat dorsal root ganglion neurons (14, 17). Thus, Bcl-2 may be more important than Bcl-x_L as a regulator of Sindbis virus-induced death in neural cells. Additional studies examining the effects of Beclin on Sindbis virus infection in mice that are deficient in Bcl-2 may help define whether Bcl-2 is the biologically important Beclin-binding partner in in vivo antiviral pathways in the CNS.

The mechanisms by which Beclin, in cooperation with Bcl-2-like proteins, functions to inhibit Sindbis virus replication and Sindbis virus-induced neuronal death are unknown. Both Semliki Forest virus and Sindbis virus have been shown to inactivate the antiapoptotic function of Bcl-2 in transfected fibroblasts through caspase-induced Bcl-2 cleavage (10). In addition, Nava et al. have shown that *crmA* increases the survival of Sindbis virus-infected mice (24), suggesting a role for *crmA*-inhibitable CNS caspase activity in the pathogenesis of fatal encephalitis. One possibility, therefore, is that binding to Beclin somehow protects Bcl-2 (or Bcl-x_L) from cleavage by caspases, thereby preventing Sindbis virus-induced cell death. A second possibility is that the Beclin–Bcl-2-like protein complex blocks an endoplasmic reticulum stress signal triggered by the Sindbis virus E2 and E1 envelope glycoproteins. One of the mechanisms by which Bcl-2 and Bcl-may inhibit apoptosis is by regulating the permeability of intracellular membranes (reviewed in reference 30). Recently, we have shown that the overexpression of the transmembrane domains of the Sindbis virus E2 and E1 envelope glycoproteins induces apoptosis in AT3 cells (15). In addition, coiled-coil proteins such as Beclin may play a role in linking membrane signal transduction events with the cytoskeleton. Thus, we speculate that Beclin, a protein which localizes to intracellular membranes, may be part of a complex with Bcl-2-like proteins that regulates signalling events initiated by Sindbis virus envelope glycoproteins in the endoplasmic reticulum.

Many similarities exist between the findings of the present study and our previous work examining the effects of Bcl-2 overexpression on the natural history of Sindbis virus encephalitis. As observed with Beclin in this study, the overexpression of Bcl-2 in virally infected neurons has previously been shown to reduce CNS apoptosis, reduce CNS Sindbis virus replication, and reduce Sindbis virus mortality (17). However, in the present study, we also identify one significant biologic difference between Bcl-2 and Beclin; namely, Beclin can exert pro-

tective effects against infection by a neurovirulent strain of Sindbis virus that is known to overcome the protective effects of Bcl-2. Ubol et al. demonstrated that a histidine substitution for wild-type glutamine at position 55 of the Sindbis virus E2 envelope glycoprotein was sufficient to enable the virus to kill cells expressing Bcl-2 (41). Similarly, we have previously found that Bcl-2 expressed in a strain of Sindbis containing a glutamine at position 55 (strain 633) protects against fatal encephalitis (17), but in the present study, we found that Bcl-2 expressed in a strain of Sindbis containing a histidine at position 55 (strain TE12) confers no protection against fatal disease. Yet, when expressed in an E2-55 histidine-containing background strain of Sindbis virus, Beclin confers significant protection. Thus, the mutation in E2, which confers neurovirulence, can counter the protective effects of Bcl-2 but not of Beclin.

Several explanations have been proposed to explain the ability of the E2-55 histidine mutation to confer resistance to Bcl-2 protection against Sindbis virus-induced death. Ubol et al. suggested that the neurovirulent mutation in E2 might somehow alter either a direct interaction between E2 and Bcl-2 in the endoplasmic reticulum or a possible effect of Bcl-2 on E2 protein folding or posttranslational modifications (41). More recently, Grandgirard et al. raised the possibility that the mutation in E2 facilitates the access of caspases to Bcl-2 and subsequent triggering of Bcl-2 cleavage (10). If viral activation of caspase-induced cleavage of Bcl-2 does prove to be an important mechanism of neurovirulence of Sindbis virus strains containing E2-55 histidine, our data suggest that Beclin may serve as an important host defense factor against this strategy of neurovirulence. This hypothesis is based on the ability of Beclin, a Bcl-2-interacting protein, to protect against neuronal death induced by the TE12 strain of Sindbis virus.

Our findings suggest that the antiviral effects of Beclin observed in Sindbis virus-infected mouse brains may be exerted at a stage of viral replication after viral RNA synthesis. At 2 days after chimeric virus infection, Beclin overexpression was associated with a 50-fold reduction in viral titers but no reduction in the number of viral RNA-positive cells. This finding suggests a block or abnormality at the level of either translation of the Sindbis virus structural proteins, posttranslational modifications of viral glycoproteins, virus assembly, or budding. This observation contrasts with previous studies examining the effects of Bcl-2 on infection with a related alphavirus, Semliki Forest virus (34). On the basis of in situ hybridization studies for viral RNA and immunostaining for viral proteins, Scallan et al. concluded that *bcl-2* functions at an early stage of the virus life cycle, either entry, pretranscriptional events, or transcription, to inhibit Semliki Forest virus replication (34). The discrepancy between the findings of Scallan et al. and those reported in the present study may reflect fundamental differences between the antiviral effects of Beclin and Bcl-2, differences between Sindbis virus and Semliki Forest virus, or differences between the cell types infected. Alternatively, it is possible that Bcl-2 and/or Beclin act at multiple overlapping stages of the alphavirus life cycle and that different experimental designs in the two studies uncovered effects on different phases of replication. Given the lack of antiviral activity of Beclin lacking the Bcl-2-binding domain, it seems likely that the mechanisms by which Beclin and Bcl-2 inhibit Sindbis virus replication in mouse brain are similar.

The results of the present study do not permit us to evaluate whether the beneficial effects of Beclin on Sindbis virus-induced mortality are a consequence of antiviral effects, antiapoptotic effects, or a combination of both. It is not known whether Beclin prevents neural cell death solely as a consequence of reducing Sindbis virus replication in neurons or whether Beclin exerts antiapoptotic effects independently of its effects on viral replication. Further studies examining the effects of Beclin on apoptotic death in response to nonviral stimuli will be necessary to determine whether Beclin, like Bcl-2, functions as a general apoptosis inhibitor. If so, structure-function analyses of Beclin may be helpful to map domains important for antiviral and antiapoptotic function and to identify whether these two properties are interrelated or independent.

Previously, based on our observations with Bcl-2 and Sindbis virus infection, we postulated that molecular links may exist between cellular regulation of viral replication and cellular regulation of apoptotic death in neurons (17). Our findings that Beclin has antiviral activity and that Beclin interacts with the cell death regulator Bcl-2 further support this hypothesis. In dividing cells, inhibition of virus-induced cell death by virally encoded cell death inhibitors such as p35 (7) and adenovirus E1B can increase viral replication (3). However, in nondividing, terminally differentiated cells such as neurons, genetic pathways may exist which permit preservation of the life of the cell, without the adverse consequence of increased total viral burden for the organism. Genes such as *bcl-2* and *beclin* that are normally expressed in mammalian neurons may be important components of such pathways.

ACKNOWLEDGMENTS

The first two authors contributed equally to this work.

We thank M. B. Soares for providing the normalized human infant brain cDNA library, Takaki Sato for providing *bcl-x_S*, *bcl-x_L*, and *bax* plasmids, Steven Greenberg and Milton Packer for helpful discussions, and Tracey Curran for secretarial assistance.

This work was supported by a James S. McDonnell Foundation Scholar Award (B.L.) and NIH grants AIO1217 (B.L.), AI40246 (B.L.), AG07218 (B.H.), AG13797 (B.H.), and AG13637 (B.H.). B.L. was supported by an American Cancer Society Junior Faculty Research Award and an Irma T. Hirschl Trust Career Scientist Award.

REFERENCES

1. **Allsopp, T. E., M. F. Scallan, A. Williams, and J. K. Fazakerley.** 1998. Virus infection induces neuronal apoptosis: a comparison with trophic factor withdrawal. Cell Death Differ. **5:**50–59.
2. **Altshul, S. F., W. Gish, W. Miller, E. W. Meyers, and D. J. Lipman.** 1990. Basic local alignment tool. J. Mol. Biol. **215:**403–410.
3. **Antoni, B. A., P. A. Sabbatini, A. B. Rabson, and E. White.** 1995. Inhibition of apoptosis in human immunodeficiency virus-infected cells enhances virus production and facilitates persistent infection. J. Virol. **69:**2384–2392.
4. **Boise, L. H., M. Gonzalez-Garcia, C. E. Postema, L. Ding, T. Lindsten, L. A. Turka, X. Mao, G. Nunez, and C. B. Thompson.** 1993. *Bcl-x_L*, a *bcl-2* related gene that functions as a dominant regulator of apoptotic cell death. Cell **74:**597–608.
5. **Cheng, E. H. Y., B. Levine, L. H. Boise, C. B. Thompson, and J. M. Hardwick.** 1996. Bax-independent inhibition of apoptosis by Bcl-x_L. Nature **379:** 554–556.
6. **Clegg, R. M.** 1992. Fluorescence resonance energy transfer and nucleic acids. Methods Enzymol. **211:**353–388.
7. **Clem, R., and L. K. Miller.** 1993. Apoptosis reduces both the in vitro replication and the in vivo infectivity of baculovirus. J. Virol. **67:**3730–3738.
8. **Friedman, L. S., E. A. Ostermeyer, E. D. Lynch, C. I. Szabo, L. A. Anderson, P. Dowd, M. K. Lee, S. E. Rowell, J. M. Boyd and M.-C. King.** 1994. The search for BRCA1. Cancer Res. **54:**6374–6382.
9. **Gordon, G. W., G.-Berry, X. H. Liang, B. Levine, and B. Herman.** 1998. Quantitative fluorescence resonance energy transfer (FRET) measurements using fluorescence microscopy. Biophys. J. **74:**2702–2713.
10. **Grandgirard, D., E. Studer, L. Monney, T. Belser, I. Fellay, C. Borner, and M. R. Michel.** 1998. Alphaviruses induce apoptosis in Bcl-2-overexpressing cells: evidence for a caspase-mediated, proteolytic inactivation of Bcl-2. EMBO J. **17:**1268–1278.
11. **Hardwick, J. M.** 1997. Virus-induced apoptosis. Adv. Pharmacol. **41:**295–336.
12. **Herman, B.** 1996. Fluorescence microscopy: state of the art, p. 1–14. *In* J. Slavik (ed.), Fluorescent microscopy and fluorescent probes. Plenum Press, New York, N.Y.

13. **Hinshaw, V. S., C. W. Olsen, N. Dybdahl-Sissoko, and D. Evans.** 1994. Apoptosis: a mechanism of cell killing by influenza A and B viruses. J. Virol. **68:**3667–3673.
14. **Jiang, H. H., and B. Levine.** Unpublished data.
15. **Joe, A. K. H. H. Foo, L. Kleeman, and B. Levine.** 1998. The transmembrane domains of Sindbis virus envelope glycoproteins induce cell death. J. Virol. **72:**3935–3943.
16. **Krakauer, D. C., and R. J. Payne.** 1997. The evolution of virus-induced apoptosis. Proc. R. Soc. Lond. Ser. B **264:**1757–1762.
17. **Levine, B., J. E. Goldman, H. H. Jiang, D. E. Griffin, and J. M. Hardwick.** 1996. Bcl-2 protects mice against fatal alphavirus encephalitis. Proc. Natl. Acad. Sci. USA **93:**4810–4815.
18. **Levine, B., Q. Huang, J. T. Isaacs, J. C. Reed, D. E. Griffin, and J. M. Hardwick.** 1993. Conversion of lytic to persistent alphavirus infection by the *bcl-2* cellular oncogene. Nature **361:**739–742.
19. **Lewis, J., S. L. Wesslingh, D. E. Griffin, and J. M. Hardwick.** 1996. Alphavirus-induced apoptosis in mouse brains correlates with neurovirulence. J. Virol. **70:**1828–1835.
20. **Liang, X. H., M. Volkmann, R. Klein, B. Herman, and B. Lockett.** 1994. Colocalization of tumor suppressor protein p53 and human papillomavirus E6 protein in human cervical carcinoma cell lines. Oncogene **8:**2645–2652.
21. **Liao, C. L., Y. L. Lin, J. J. Wang, Y. L. Huang, C. T. Yeh, S. H. Ma, and L. K. Chen.** 1997. Effect of enforced expression of human *bcl-2* on Japanese encephalitis virus-induced apoptosis in cultured cells. J. Virol. **71:**5963–5971.
22. **Lupas, A., M. Van Dyke, and M. J. Stock.** 1991. Predicting coiled coils from protein sequences. Science **252:**1162–1164.
23. **Merry, D. E., and S. J. Korsmeyer.** 1997. Bcl-2 gene family in the nervous system. Annu. Rev. Neurosci. **20:**245–267.
24. **Nava, V. E., A. Rosen, M. A. Veliuona, R. J. Clem, B. Levine, and J. M. Hardwick.** 1998. Sindbis virus induces apoptosis through a caspase-dependent CrmA-sensitive pathway. J. Virol. **72:**452–459.
25. **Oberhaus, S. M., R. L. Smith, G. W. Clayton, T. S. Dermody, and K. L. Tyler.** 1997. Reovirus infection and tissue injury in the mouse central nervous system are associated with apoptosis. J. Virol. **71:**2100–2106.
26. **Olsen, C. W., J. C. Kehren, N. R. Dybdahl-Sissoki, and V. S. Hinshaw.** 1996. *bcl-2* alters influenza virus, yield, spread, and hemagglutinin glycosylation. J. Virol. **80:**663–666.
27. **Oltvai, Z., C. L. Milliman, and S. J. Korsmeyer.** 1993. Bcl-2 heterodimerizes in vivo with a conserved homolog, Bax, that accelerates programmed cell death. Cell **74:**609–619.
28. **Park, J. R., and D. M. Hockenbery.** 1996. Bcl-2, a novel regulator of apoptosis. J. Cell. Biochem. **60:**12–17.
29. **Pekosz, A., J. Phillips, D. Pleasure, D. Merry, and F. Gonzalez-Scarano.** 1996. Induction of apoptosis by LaCrosse virus infection and role of neuronal differentiation and human *bcl-2* expression in its prevention. J. Virol. **70:** 5329–5335.
30. **Reed, J. C.** 1997. Double identity for proteins of the Bcl-2 family. Nature. **387:**773–776.
31. **Rodgers, S. E., E. S. Barton, S. M. Oberhaus, B. Pike, C. A. G. Terence, K. L. Tyler, and T. S. Dermody.** 1997. Reovirus-induced apoptosis of MDCK cells is not linked to viral yield and is blocked by Bcl-2. J. Virol. **71:**2540–2546.
32. **Rommens, J. M., F. Durocher, J. McArthur, P. Tonin, J.-F. LeBlanc, T. Allen, C. Samson, L. Ferri, S. Narod, K. Morgan, and J. Simard.** 1995. Generation of a transcription map at the HSD17B locus centromeric to BRCA1 at 17q21. Genomics **28:**530–542.
33. **Root, D. D.** 1997. In situ molecular association of dystrophin with actin revealed by sensitized emission immuno-resonance energy transfer. Proc. Natl. Acad. Sci. USA **94:**5685–5690.
34. **Scallan, M. F., T. E. Allsopp, and J. K. Fazakerley.** 1997. *bcl-2* acts early to restrict Semliki Forest virus replication and delays virus-induced programmed cell death. J. Virol. **71:**1583–1590.
35. **Selvin, P. R.** 1995. Fluorescence resonance energy transfer. Methods Enzymol. **246:**300–333.
36. **Shen, Y., and T. E. Shenk.** 1995. Viruses and apoptosis. Curr. Opin. Genet. Dev. **5:**105–111.
37. **Soares, M. B., M. F. Bonaldo, P. Jelene, L. Su, L. Lawton, and A. Efstradiadis.** 1994. Construction and characterization of a normalized cDNA library. Proc. Natl. Acad. Sci. USA **91:**9228–9232.
38. **Tangir, J., M. G. Muto, R. S. Berkowitz, W. R. Welch, D. A. Bell, and S. C. Mok.** 1996. A 400 kb novel deletion unit centromeric to the BRCA1 gene in sporadic epithelial ovarian cancer. Oncogene **12:**735–740.
39. **Teodoro, J. G., and P. E. Branton.** 1997. Regulation of apoptosis by viral gene products. J. Virol. **71:**1739–1746.
40. **Tucker, P. C., E. G. Strauss, R. J. Kuhn, J. H. Strauss, and D. E. Griffin.** 1993. Viral determinants of age-dependent virulence of Sindbis virus for mice. J. Virol. **67:**4605–4610.
41. **Ubol, S., P. C. Tucker, D. E. Griffin, and J. M. Hardwick.** 1994. Neurovirulent strains of alphavirus induce apoptosis in bcl-2-expressing cells: role of a single amino acid change in the E2 glycoprotein. Proc. Natl. Acad. Sci. USA **91:**5202–5206.
42. **Yin, X.-M., Z. N. Oltvai, and S. J. Korsmeyer.** 1994. BH1 and BH2 domains of Bcl-2 are required for inhibition of apoptosis and heterodimerization with BAX. Nature **369:**321–323.